Materials Today Bio 31 (2025) 101618

Contents lists available at ScienceDirect

Materials Today Bio

journal homepage: www.journals.elsevier.com/materials-today-bio

Age-tailored artificial skin model for cosmetic film development

Marta Gonçalves [a,b,c,1], Sofia Brito [b,c,d,1], Chaeyeon Song [e], Youngkyu Han [e], Bum-Ho Bin [f], Byung Mook Weon [b,c,g,*]

[a] School of Chemical Engineering and Global Research Center for e-Chem Meditronic Systems, Sungkyunkwan University, Suwon, 16419, South Korea
[b] Research Center for Advanced Materials Technology, Sungkyunkwan University, Suwon, 16419, South Korea
[c] School of Advanced Materials Science and Engineering, Sungkyunkwan University, Suwon, 16419, South Korea
[d] Department of Pharmacology, College of Medicine, The Catholic University of Korea, Seoul 06591, South Korea
[e] AMOREPACIFIC Research and Innovation Center, Yongin, 17074, South Korea
[f] Department of Biological Sciences, Ajou University, Suwon, 16499, South Korea
[g] Xgraphy Inc., Suwon, 16419, South Korea

ARTICLE INFO

Keywords:
Aging skin
Artificial skin
Cosmetic
Thin film
Biomimetics
Soft materials

ABSTRACT

Thin film deposition is essential in the cosmetic industry, where formulations such as foundations and concealers rely on uniform layer formation to conceal pores and texture irregularities for a natural and even appearance. However, variations in skin topography, influenced by factors such as aging, genetics, and environmental exposure, can significantly affect the behavior of these films. Aging, in particular, leads to increased skin roughness and wrinkles, creating challenges to achieve consistent cosmetic deposition in diverse age groups. This study investigates the impact of age-related topographical changes on cosmetic thin film deposition and introduces a model for standardized, age-specific evaluation of cosmetic performance. Using X-ray microtomography, we compare skin topography from a cohort of the Korean population segmented into young and aged groups. A PDMS-based model is then constructed using these skin topographies, and thin film deposition is assessed both on human-derived skin positives and on the assembled model. This approach demonstrates the potential of artificial skin models for the precise quantification and evaluation of film coverage. In addition, we propose an improved model that incorporates key factors such as skin porosity and sebum production to increase realism. By exploring the interactions between skin morphology and cosmetic behavior, this method offers valuable insights into optimizing formulations to meet the diverse needs of consumers.

1. Introduction

Thin film deposition is a pivotal process in various industries, including electronics, coatings, biologics, and pharmaceuticals, where precise and controlled layer formation is essential to achieve optimal performance and functionality [1–4]. In the cosmetic industry, thin film deposition is critical for product performance, as formulations such as foundations and concealers rely on uniform deposition. These films improve the appearance of the skin by concealing topographical variations, such as pores and textural irregularities, thereby achieving the even natural appearance desired by consumers [5–7]. As the global cosmetic market continues to expand, valued at $374.19 billion in 2023 and projected to reach $758.05 billion by 2032, according to Fortune Business Insights, the demand for improved cosmetic formulations that improve coverage, adhesion, and durability is also increasing [8]. Effective cosmetic thin film formation depends on the chemical composition of each formulation and the structural attributes of the skin substrate, as deposition behavior is significantly affected by skin-cosmetic interface variables such as roughness and topography [9]. Achieving optimal coverage and adhesion requires an in-depth understanding of these interactions to produce formulations that are tailored for various skin types. To this end, it is essential to establish advanced and standardized evaluation methods to assess thin film deposition on the skin. Implementing such methodologies will enable precise and reproducible assessments of cosmetic film performance across diverse skin types, ultimately driving innovations that meet the high expectations of both industry standards and consumer demands [10,11].

Skin topography varies among individuals, which can significantly

* Corresponding author. School of Advanced Materials Science and Engineering, Sungkyunkwan University, Suwon 16419, South Korea.
E-mail address: bmweon@skku.edu (B.M. Weon).
[1] M.G. and S.B. contributed equally to this work.

https://doi.org/10.1016/j.mtbio.2025.101618
Received 21 December 2024; Received in revised form 14 February 2025; Accepted 25 February 2025
Available online 26 February 2025

impact thin film deposition. A significant factor driving changes in skin structure is aging, a natural process marked by a decline in biological functions [12,13]. Skin aging can also be influenced by genetic predisposition, hormonal changes, and environmental factors such as UV exposure and air pollution, which accelerate the aging phenotype [14,15]. These factors result in a decrease in cell turnover, leading to increased roughness and scaliness. In addition, loss of elastin fibers and collagen degradation contribute to the formation of wrinkles [16]. The contrast between the smooth texture of youthful skin and the deep wrinkles and roughness of aged skin substantially alters cosmetic film deposition. Since the deposition of cosmetic films is expected to vary widely between individuals of different ages, tailoring cosmetic testing platforms to incorporate age-specific characteristics and developing standardized evaluation methods can offer a valuable approach to developing and evaluating cosmetic performance across diverse age groups (Fig. 1). By replicating the unique morphological and physiological characteristics of the skin in different stages of life, this strategy can enhance the precision of cosmetic product formulations for varying skin types. Furthermore, such platforms could have broader applications in industries reliant on skin-related thin film deposition, including biomimetics and drug delivery systems, improving the performance and adaptability of related technologies [17]. In this study, we examined the topographical variations in the skin during aging to develop a model for a standardized age-differentiated analysis of cosmetic thin film deposition, applicable for a wide array of cosmetic performance tests. The substrate was further upgraded to include factors such as skin porosity and sebum production to increase the realism of the model. Furthermore, by employing X-ray microtomography, precise quantification of cosmetic profiles and statistical analysis of coverage could be achieved [18,19]. By understanding the interaction between skin morphology and cosmetic product behavior, the cosmetic industry can optimize formulations to improve film deposition and long-lasting wear, addressing the diverse needs of consumers and strengthening their market position. This approach highlights the importance of integrating comprehensive skin models and advanced imaging techniques into product development, enabling the creation of formulations tailored to diverse skin types and ages. By offering a reliable alternative to animal testing, this strategy supports the development of more effective, inclusive, and ethically responsible solutions.

2. Experimental section

To investigate the influence of skin topography on cosmetic film performance, age-tailored artificial skin models were developed based on a three-step approach (Fig. 2). Step 1) The morphological differences between young and aged skin were quantified using positive skin prints, which were generated from negative prints of human forehead imprints to capture structural variations. Step 2) These characteristics were then used to create artificial skin models that mimic the topographical features of each age group. Step 3) The artificial skin models were subsequently validated for cosmetic film testing, where formulations with distinct properties were applied to assess film coverage, offering insights into the influence of skin texture on product performance. A comprehensive description of the experimental procedures is presented in the following sub-sections.

2.1. Acquisition of skin prints

Skin prints were obtained from a cohort of Korean subjects comprising two distinct groups: a "young" group of 12 subjects aged between 20 and 30 years and an "aged" group of 12 subjects aged between 50 and 60 years. The subject group comprised an equal number of female and male volunteers. Data analysis was performed based on age, without considering sex, as no significant variations could be identified for the variables under study. Skin negative prints were prepared *in vivo* using Body Double^{TM} (Smooth On Inc., United States), a biocompatible silicone, according to the manufacturer's instructions. Briefly, the two components of the kit were mixed in equal parts and applied to the clean forehead of the subjects approximately at a dimension of 2 × 5 cm and left to dry for 20 min. To obtain skin-positive prints, Dragon Skin^{TM}

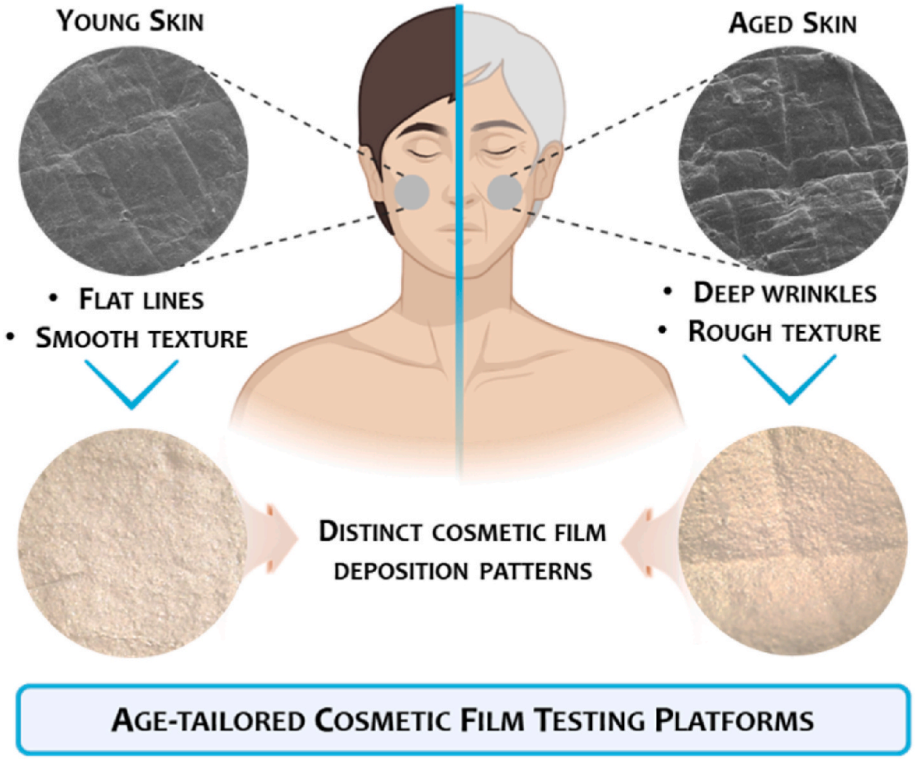

Fig. 1. Schematic representation depicting the main topographical differences between young and aged skin and the necessity for age-differentiated platforms.

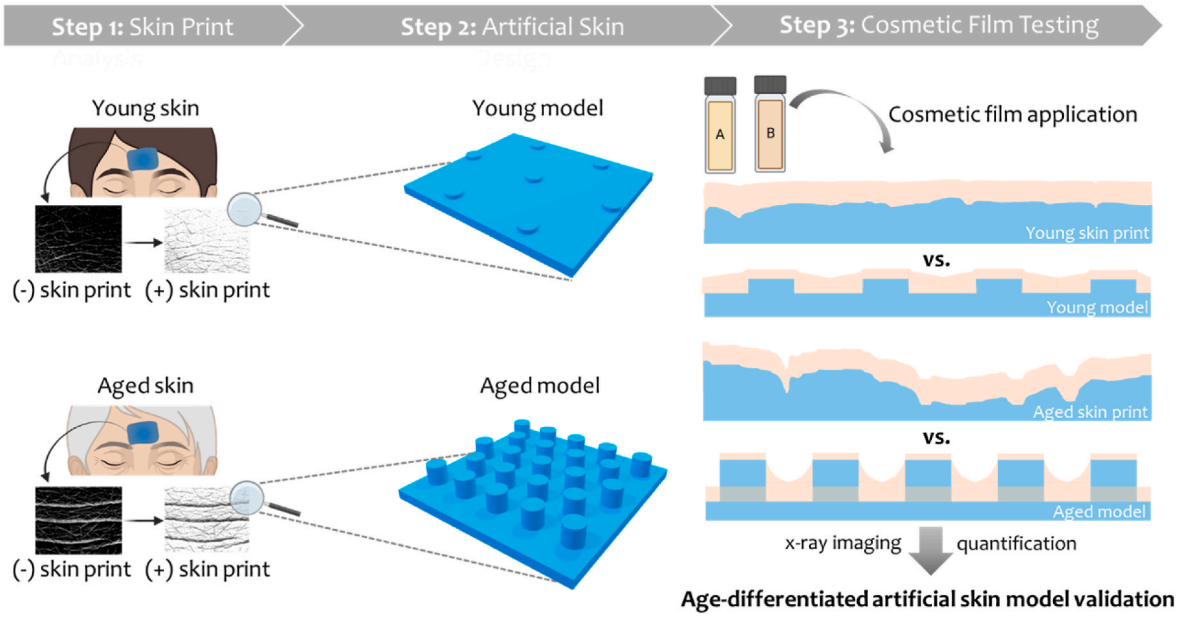

Fig. 2. Overview of the methodology to develop and employ an age-differentiated artificial skin model for cosmetic film testing. Step 1: Acquisition of negative (−) skin prints from young and aged human foreheads as a mold to cast positive (+) skin prints that are subjected to structural analysis. Step 2: Design of the age-differentiated artificial skin models based on the analyzed properties of the positive skin imprints. Step 3: Testing cosmetic products with distinct formulations (i.e. A vs. B) to validate the proposed system for cosmetic film analysis. Schematic illustration not to scale.

(Smooth On Inc., United States) was prepared according to the manufacturer's instructions and poured over the previously obtained negative prints that were fixed to 60 mm Petri dishes (SPL Life Sciences, South Korea). The samples were degassed for 2 h to remove trapped bubbles and left to dry for 6 h at room temperature. The samples were then cut into 1 × 1 cm square pieces with a razor blade for further analysis. To characterize the topographical differences between the young and aged groups, the wrinkle height and the wrinkle pitch were the chosen parameters for quantification.

2.2. Artificial skin substrate fabrication

The artificial skin substrate was fabricated with SYLGARD^{TM} 184 Silicone Elastomer Kit (Dow, United States), a two-component system (polymeric base, curing agent) mixed in a 20:1 ratio that resulted in a formed composite of polydimethylsiloxane (PDMS). To achieve a surface that mimics the natural texture of human skin, a micropillar design was adopted with two different configurations based on the skin prints' topographical parameters quantification: (I) Young model - cylindrical pillars with diameter (D) = 100 μm and height (H) = 25 μm spaced by a pitch (P) = 400 μm; (II) Aged model - cylindrical pillars with diameter (D) = 100 μm and height (H) = 100 μm spaced by a pitch (P) = 100 μm. The designs were etched on silicon wafer master molds and treated with a hydrophobic coating to help with the release of the polymeric substrate. The PDMS mixture was poured into the master molds and placed in a vacuum-degassing chamber until all trapped bubbles were released. The substrate was left to cure in a convection oven at 75 °C for 4 h, followed by a cooling period, and then gently peeled off the silicon wafer. The samples were then cut into 1 × 1 cm square pieces with a razor blade for further analysis. The manufacturing of porous artificial skin substrates follows a similar methodology, and the porous inclusion procedure is explained in more detail in the Results and Discussion section [20].

2.3. Cosmetic thin film deposition

Two cosmetic foundation products, advertised, respectively, as low and high coverage formulations, were selected from the market to test their different coverage capacities on young and aged skin. The distinction between the two formulations arises from differences in composition, such as the content of powders, polymers and emulsifiers, as well as the type and ratio of incorporated oils. These compositional variations influence the rate of solvent evaporation and the kinetics of makeup film formation. The "low coverage" formulation includes both chemical and physical sunscreen agents, acrylate and silicone polymers (film formers) to aid with longevity and water resistance, and polymers that help with oil absorption for a smoother finish. This long-wear formulation is expected to apply smoothly and thinly along the surface of the skin. The "high coverage" formulation has a higher content of physical mineral filters, which are responsible for the increase in opacity. Furthermore, besides multiple silicone and polymeric film formers for long-wear coverage, this formulation has spherical filler powders (i.e. PMMA, Nylon-12) that contribute for matte finishes and increased "soft-focus" effect. Therefore, this formulation is expected to fill in the skin texture, giving a long-lasting smooth appearance. The formulations were applied to 1 × 1 cm squared sections of both skin prints and micropillar artificial skin models using a spin-coater set to 1750 RPM for 60 s. This technique was used to achieve a thin film deposition that closely replicates the average application speed of cosmetic products to the skin surface. The samples were subsequently imaged after ensuring complete drying of the cosmetic film.

2.4. X-ray computed microtomography

X-ray computed microtomography was utilized to visualize and quantify the characteristics of skin prints and artificial skin models. The experiments were carried out at the Pohang Light Source II (PLS-II) - 6C Biomedical Imaging (BMI) beamline in South Korea. This beamline is characterized by phase contrast imaging with a monochromatic hard X-ray source. The samples were analyzed using an energy of 37 keV to ensure complete imaging, as the sample size exceeded the field of view. This approach was necessary to prevent damage that could result from cutting the samples. The field of view was 1.70 × 1.40 mm^2 (pixel size: 0.65 μm). The detailed image acquisition process is described in previous reports [21,22]. The acquired three-dimensional data sets were visualized and analyzed using Avizo visualization software

(ThermoFisher Scientific, United States). This allowed volume reconstructions and the visualization of 2D cross-sections in multiple directions for quantitative analysis.

2.5. Scanning electron microscopy

Additional imaging was achieved with scanning electron microscopy (SEM) (S-3000H, Hitachi, Japan) taken at 10 kV. Since the sample is nonconductive, it was coated with gold for 60 s using a gold sputter (E−1010 Ion Sputter, Hitachi, Japan) prior to imaging.

2.6. Cosmetic film performance analysis

To evaluate the drying dynamics of the cosmetic formulations under study, mass was automatically measured every 30 min during 24 h utilizing an electronic mass balance (EX224G, Ohaus, United States). All drying experiments were conducted at 20 ± 2 °C temperature and 20 ± 5% relative humidity. To visualize the temporal evolution of cosmetic drying after spin-coating and the wear of the film before and after performance tests, a digital upright microscope (VHX-700FE, Keyence, Japan) was utilized. For a transfer test, the two formulations were deposited with spin-coating and allowed to settle for 1 h. Subsequently, a cut-out of the inner layer of a face mask was gently pressed against the cosmetic film for 2 s, in both young and aged models. For further image processing and analysis, such as surface roughness measurements and area quantification, the Fiji software and respective bundled plugins were used. The contact angle measurements were obtained from side-view optical images acquired with a drop shape analyzer by dropping a 5 μL droplet of deionized water on the cosmetic films (DSA25, Krüss, Germany). After spin-coating the cosmetic formulations onto the artificial skin, the contact angle was measured at 30 min, 60 min, and 24 h after deposition. For a water resistance test, a static and an active immersion experiment was conducted. For the static immersion, artificial skin models coated with a spin-coated cosmetic film were submerged in a petri dish with deionized water for 30 min. For the active immersion, the samples were submerged with deionized water in a tube, later positioned in a digital roller shaker (Roller 6, IKA, Germany) to agitate for 30 min at a 40 RPM. While these tests do not encompass the full diversity of real-world variables, they offer a comparative approach for a quantitative assessment of cosmetic film deposition of variable formulations in skins of variable morphologies, while ensuring reproducibility in a controlled experimental setting [23].

2.7. Statistics and reproducibility

To quantify the topographical characteristics of skin positive prints, the samples collected from each individual were measured in at least n = 5 replicates for each parameter. The thickness of the cosmetic film was measured for each sample group in n = 15 replicates to quantify the coverage of the cosmetic film. Graphs were plotted as relative fold changes to each corresponding maximum to compare skin positives with skin models. *P*-values were determined utilizing a one-way ANOVA with a Tukey test. Graphs were plotted as relative fold changes to each age group's maximum to analyze porous skin models. *P*-values were determined utilizing unpaired two-tailed Student's t-tests. For all data, statistical differences were defined as $*P \leq 0.05$; $**P \leq 0.01$; $***P \leq 0.001$. All the aforementioned statistical analyses were performed using Origin 2017. Data collection and analysis were not performed blind to the conditions of the experiments.

3. Results and Discussion

3.1. Development of age-tailored artificial skin models

The skin comprises distinct layers: the epidermis, dermis, and subcutaneous tissue. The epidermis, as the outer layer, is primarily responsible for the texture and morphology of the skin, forming a critical barrier to protect the body from external threats [24,25]. The dermis is responsible for the synthesis of collagen and elastin, which impart structural integrity and elasticity to the skin [26,27]. In addition, skin appendages, including hair follicles and sebaceous glands, contribute to the formation of pores and the accumulation of sebum, a lipid-rich substance that aids in maintaining hydration and provides a protective barrier against microbial invasion [28]. Despite continuous cellular turnover, the skin structure remains dynamic and adapts to internal and external stimuli.

To develop age-specific artificial skin models that accurately replicate the topographical features of both young and aged human skin, we initially focused on simulating surface topography changes associated with aging [29–32]. This approach is based on the understanding that the rate of cellular turnover in the epidermis and dermis plays a role in the formation of wrinkles and increased skin roughness over time. To do so, skin prints were collected from two distinct age groups: a "young" group (aged 20–30 years) and an "aged" group (aged 50–60 years). The collected skin prints were subjected to X-ray microtomography analysis to obtain data regarding two parameters: wrinkle height (W_h) and wrinkle pitch (W_p). W_h is defined as the vertical distance from the lowest point of a wrinkle to the skin's baseline, while W_p refers to the distance between adjacent wrinkles. An example of these measurements is shown in Fig. 3A, where 2D cross-sectional images, obtained via X-ray microtomography, provide *in-situ* side view of the skin prints without physical damage to the substrate. The three-dimensional reconstructions and side-view cross-sections were taken from the skin prints of all participants, with an average of 60 measurements per age group for each parameter. The relative frequency distribution of the measurements is also illustrated in Fig. 3B for each age group. The data is organized into bin sizes appropriate to the order of magnitude of the measurements. The W_h exhibits variability at the order of tens, therefore the bin size is 10. For the W_p, the variability is present at the order of hundreds, resulting in a bin size of 100. This granularity captured biologically relevant variations, enabling precise analysis and the identification of common structural characteristics. To account for the heterogeneous nature of human skin, the most frequent measurement ranges were selected, ensuring a realistic mimetic model. An example of this heterogeneity is the occasional presence of deeper wrinkles (see Supplementary Data Fig. S1) that greatly deviate the measurements average, hence the choice being made based of the measurements range frequency. The bars corresponding to these ranges are highlighted in the plots, serving then as a guideline for designing the artificial skin models. For young skin, characterized by a smoother surface, the highest relative frequency for W_h was between 20 and 30 μm, and for W_p between 300 and 500 μm. In contrast, for aged skin, characterized by a rougher texture with more visible wrinkles, the highest relative frequency for W_h was between 80 and 120 μm, and for W_p between 0 and 200 μm. These results are consistent with previous reports on wrinkle depth measurements across different age groups [31,33]. Particularly, X-ray microtomography enabled direct imaging of cross-sectional slices with sub-micron resolution, providing a highly accurate methodology for assessing skin roughness. Based on these results, two micropillar designs were created to reflect and mimic similar topographical properties to both young and aged skin, by varying the height and the pitch of the pillars. Maintaining the pillar diameter fixed at 100 μm, the young model was designed with pillars with a height of 25 μm spaced by a pitch of 400 μm, and the aged model was designed with pillars with a height of 100 μm spaced by a pitch of 100 μm.

3.2. Characterization of age-tailored artificial skin models

The designed platforms were used to fabricate artificial skin substrates, facilitating easy and reproducible topographical replication. To this end, PDMS, a transparent silicone polymer material with high biocompatibility and moldability, was utilized. The young and aged skin

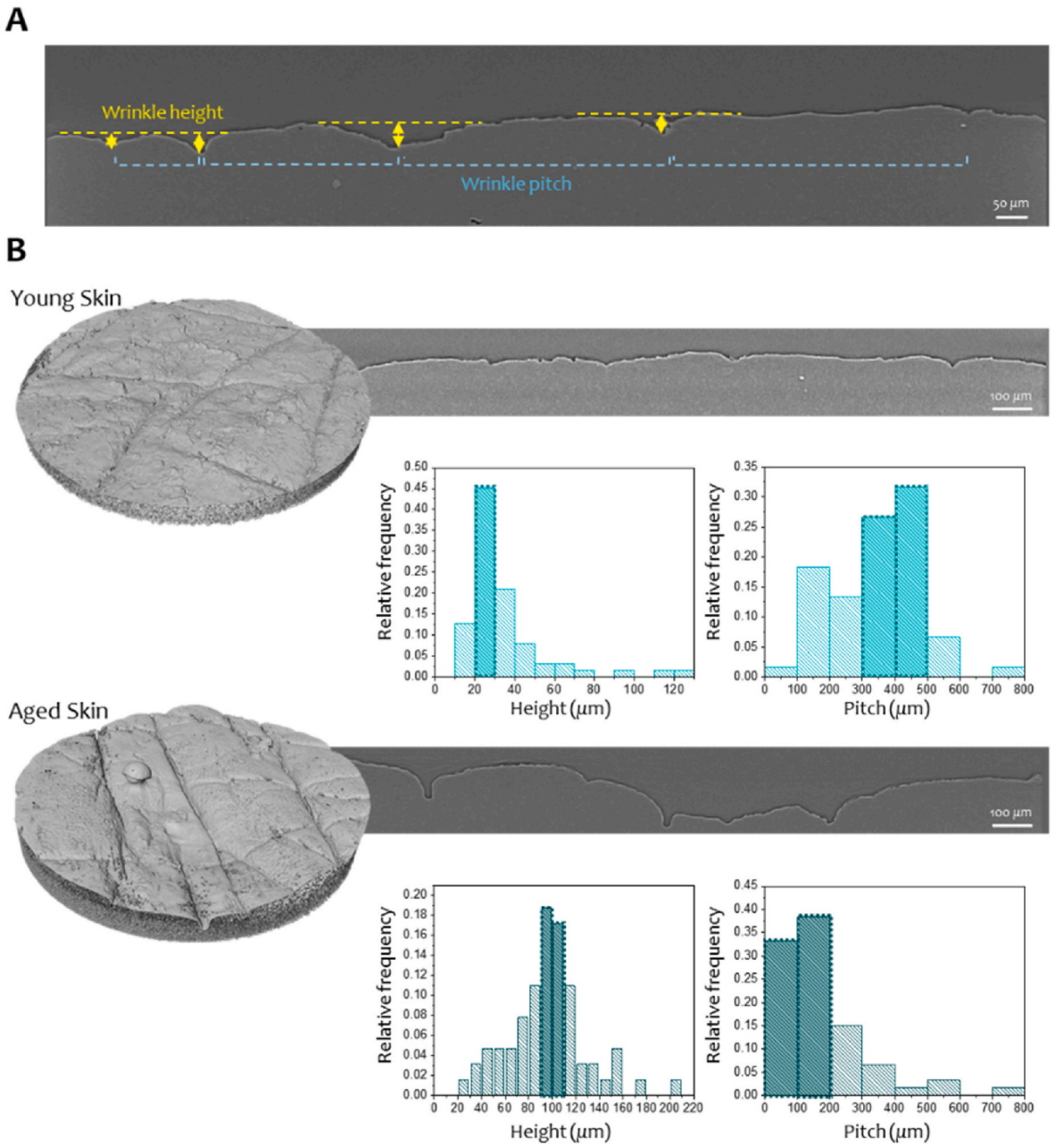

Fig. 3. Human skin print analysis. (A) Schematic illustration of the measurements taken in a representative X-ray cross-section view of a human skin print. (B) Quantification of wrinkle height and pitch from young and aged skin prints analyzed by X-ray microtomography.

models were then produced in large batches and divided into 1 cm × 1 cm squares (Fig. 4A) for all experiments, a size suitable for visualization with various devices and compatible with the cosmetic application by spin coating, ensuring consistent results. Fig. 4B presents SEM micrographs, which highlight the differences in pillar height and spacing between young and old skin models, as previously designed in Fig. 2. SEM further confirmed that age-specific designs were accurately imprinted onto the PDMS substrates, with no defects observed during casting or release.

For precise measurement of the substrate dimensions, X-ray imaging was utilized. Computed microtomography enabled *in situ* non-invasive visualization of the internal structures of the substrate in three dimensions, as well as the generation of two-dimensional orthogonal slices in any direction. Fig. 4C represents the three-dimensional reconstruction and the two-dimensional cross-sectional X-Z slices of the pillar arrangement for both the young and the aged model, where direct measurements confirm the dimensions to be in the representative range decided for each age-differentiated model.

The artificial skin model developed in this study offers significant advantages over conventional models that rely on replicas of skin topography, which are often subject to high variability [34,35]. Our model not only provides a more standardized surface, minimizing inconsistencies associated with natural skin replicas, but is also age-differentiated, enabling customized studies that reflect the unique characteristics of skin at different stages of life. This combination of standardization and age specificity ensures greater reproducibility in experimental results and makes the model particularly suitable for consistent, reliable, and ethical analyses of cosmetic film deposition across diverse age groups.

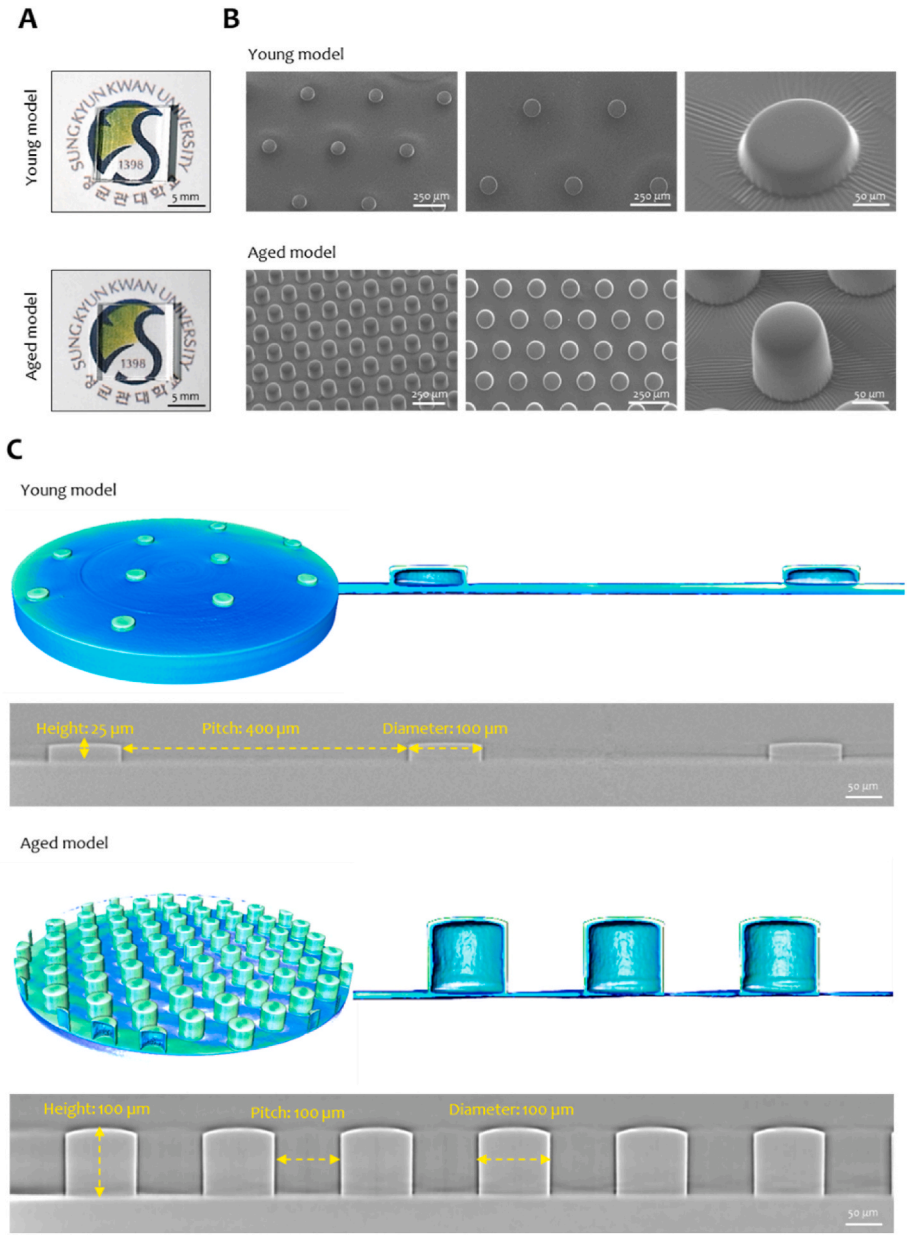

Fig. 4. Artificial skin model characterization. (A) Digital photographic representation of the young and aged artificial skin models. (B) SEM micrographs of the young and aged skin models with increasing magnifications. (C) X-ray 3D reconstructions and X-Z cross-sectional slices of young and aged artificial skin models with respective measurements.

3.3. Model validation by assessment of cosmetic film coverage

An age-differentiated artificial skin model offers significant potential for predicting how cosmetic products interact with skin of varying topographies, thus aiding in the creation of age-targeted formulations. To validate the proposed artificial skin model, a thin layer of two distinct cosmetic formulations ("low" and "high" coverage) was applied to both the skin prints and the artificial skin models. This aimed to assess the applicability of the artificial skin models as substitutes for *in vivo* testing during product development. A preliminary SEM imaging analysis confirmed that the distinct formulations appeared to show different deposition patterns, though their precise visualization and quantification proved difficult with this approach (see Supplementary Data Fig. S2). For the obtention of high-quality and quantifiable image data, X-ray microtomography was utilized to generate three-dimensional reconstructions and two-dimensional cross sections of each skin print or artificial skin model. It is important to note that, given the safety constraints of *in vivo* X-ray imaging, skin positive prints were selected as a comparative tool for evaluating cosmetic film coverage and determining the structural and topographical resemblance of the artificial skin models to real human skin. The selected skin prints were chosen from the subject pool as representative individuals whose skin topography falls within the highest frequency measurement range previously discussed in Fig. 3B. In both young skin and the model, the surface texture was not highly pronounced. Thus, the application of a low coverage formulation resulted in a smooth and even cosmetic film appearance both in the young and skin and young model. This is supported by both the three-dimensional reconstructions and the two-dimensional cross-sectional side views. In contrast, in the aged skin and model, the same thin, low coverage cosmetic film was unable to conceal the natural texture of the skin. The three-dimensional reconstructions and the two-dimensional cross sections distinctly demonstrate the uneven appearance of the surface, where the natural roughness of the skin remains dominant. In addition to direct

visualization, X-ray imaging also enables quantification of several parameters to characterize these models in a more systematic way [10]. From the side-view images in Fig. 5A, the thickness of the cosmetic film was measured at various points to understand the variations between young and aged skin (Fig. 5B). The results show that the normalized coverage of the cosmetic film was significantly different between young and old skin, the coverage being lower for the latter group. Furthermore, the results also show that the coverage measurements for the skin prints and the designed models were not significantly different within each age group, corroborating the model validity in replicating the behavior of real human skin. Film thickness is a parameter often taken into account when addressing the formation and performance of cosmetic films, particularly in long-wear cosmetics such as foundation formulations, hence the advantage of the proposed method that allows direct quantification of this parameter [36,37]. In addition, the total length of the coverage line was also measured (Fig. 5C). These results show that, due to the more irregular surface of the aged skin and model, the total length of the coverage surface line was higher, showing the inability of the cosmetic film to mask the irregularities of the surface and still displaying the natural waviness of the older skin's topography. Since surface roughness is a critical parameter that affects cosmetic adhesion to the skin and this parameter is shown to have age-dependent differences, the creation of a facile method for accurate prediction of cosmetic film deposition is expected to greatly benefit formulation development in a

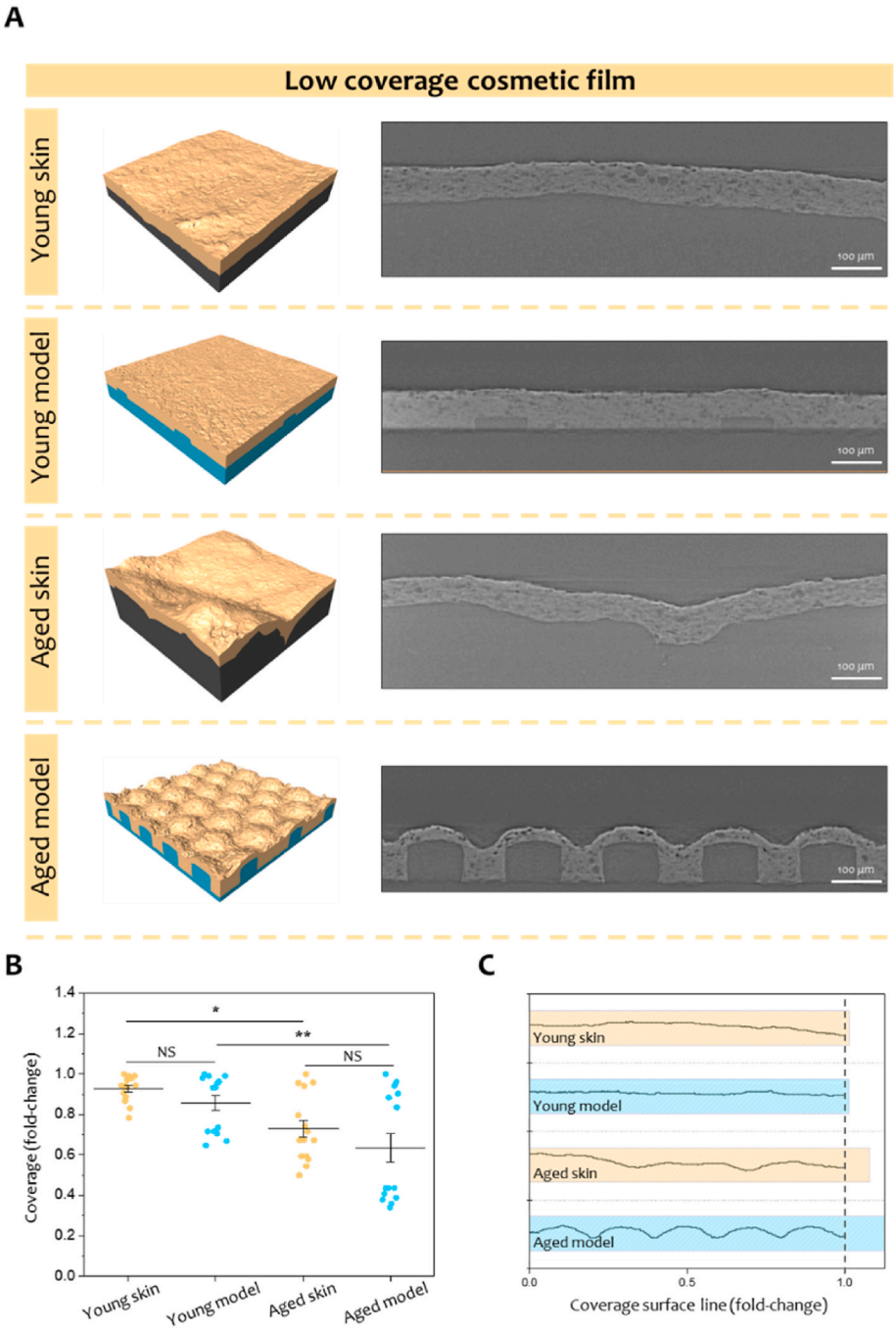

Fig. 5. Low coverage cosmetic film analysis. (A) Representative X-ray 3D reconstructions and X-Z cross-section slices of cosmetic film coverage in young and aged skin in comparison with young and aged models. (B) Quantification of coverage thickness from X-Z cross section slices. (C) Representation of coverage profile and quantification of total coverage surface line length.

systematic way [9,38].

To verify the applicability of the designed artificial skin model to distinguish and characterize cosmetic products with distinct formulations, the high coverage cosmetic formulation was also applied to both young and aged skin prints and skin models, as represented in Fig. 6A. Here, in contrast to what was observed for the low coverage formulation, the cosmetic film was able to provide a smooth appearance to the skin surface for both young and aged samples. The three-dimensional reconstructions and the two-dimensional cross sections both show a much more uniform surface after the high coverage formulation was applied in comparison to the low coverage formulation observed in Fig. 5A. Similarly, coverage quantification (Fig. 6B) and coverage surface line length (Fig. 6C) now show that there were no significant differences between young and aged skin and their respective models, highlighting the differences between the purpose and effect of the different cosmetic formulations. Therefore, these artificial skin models also show the potential to be used as a platform to identify the influence of cosmetic thin film application on wrinkle alleviation effects [7].

The age-tailored artificial skin substrates presented herein demonstrated strong comparability and enabled systematic, quantifiable analysis. However, it is important to note that the current study was conducted exclusively with a Korean population, which presents a limitation and underscores the potential for the development of region-specific models in the future. Furthermore, adjusting the height and

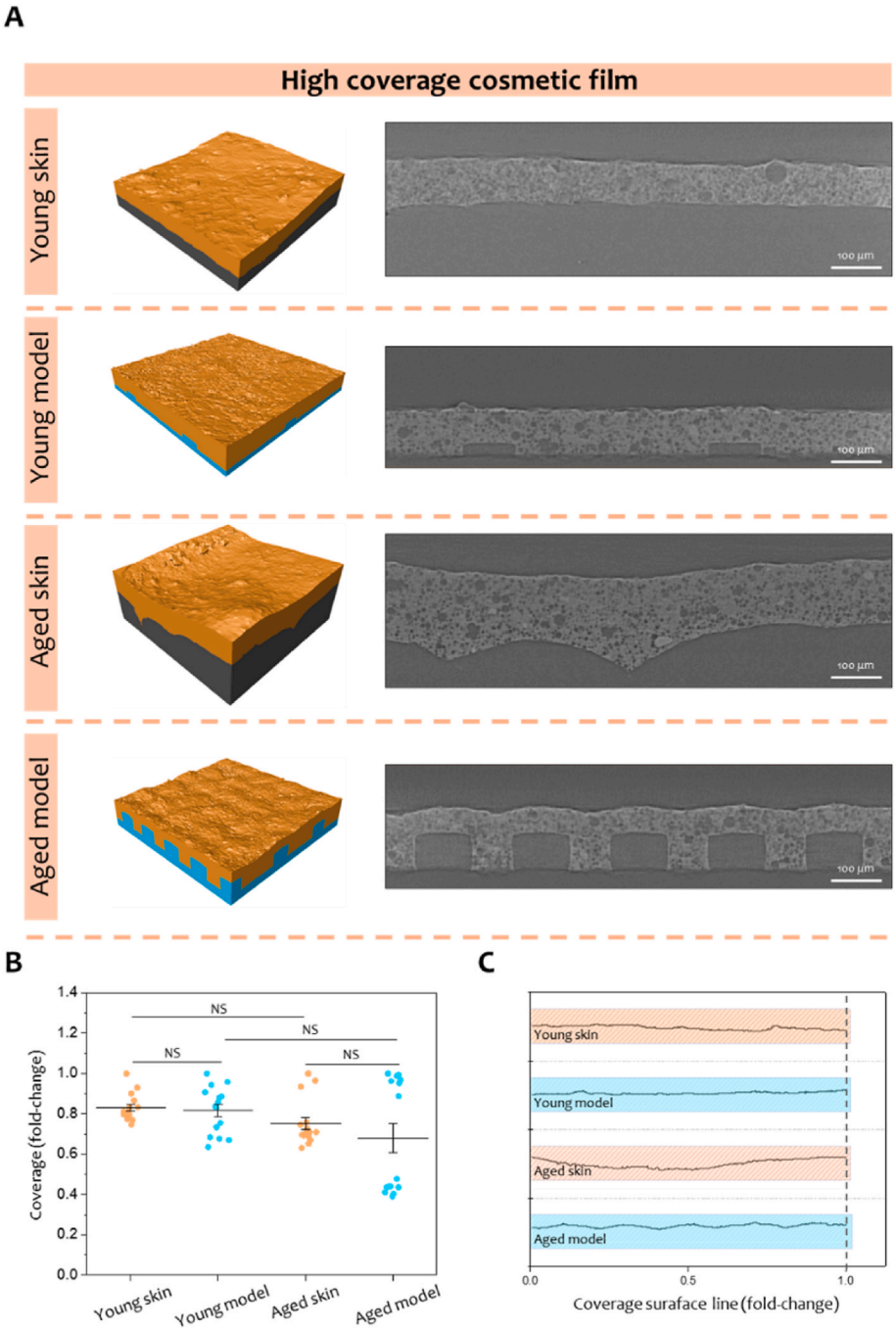

Fig. 6. High coverage cosmetic film analysis. (A) Representative X-ray 3D reconstructions and X-Z cross-section slices of cosmetic film coverage in young and aged skin in comparison with young and aged models. (B) Quantification of coverage thickness from X-Z cross section slices. (C) Representation of coverage profile and quantification of total coverage surface line length.

pitch of the pillar based on individual characteristics could serve as a promising strategy to create customized cosmetic products tailored to different skin profiles. Although this study primarily focused on the development of skin models for cosmetic film analysis, the biocompatibility of PDMS opens avenues for the advancement of these age-specific models into biohybrid artificial skin constructs incorporating other biological components, such as skin cells culture for the development of full-thickness models. Such an approach would enhance the realism of the models, facilitating the exploration of novel parameters, such as the efficacy of topical or transdermal treatments at the cellular level [39].

3.4. Characterization of cosmetic film performance in age-tailored artificial skin models

To further understand the applicability of the artificial skin models, cosmetic film performance was assessed through film adhesion (Fig. 7) and water resistance (Fig. 8) analyses [36,40,41]. Firstly, to understand the adhesion behavior of the formulations, the evaporation rate was determined by measuring the decrease in mass over time. The evaporation rate of both formulations followed a similar linear trend, with a dynamic phase during the first 400 min (approximately 7 h), reaching a plateau of roughly constant mass, indicating the film's stability (Fig. 7A). However, the low coverage formulation exhibited a higher evaporation rate compared to the high coverage formulation, as shown by the normalized mass loss measurements over time. Notably, the low coverage film resulted in a lower final mass than the high-coverage counterpart, likely due to differences in water content and the presence of a greater proportion of volatile components. To visualize how the evaporation dynamics influence film adhesion, the evolution of film morphology over time was evaluated in Fig. 7B based on the behavior exhibited in Fig. 7A, highlighting differences in structural integrity and homogeneity between the young and aged skin models. Initially, the formulation spread uniformly across both models; however, as time progressed, the aged model exhibited a more irregular pattern, with increased surface heterogeneity and localized disruptions, particularly in the low coverage cosmetic film. Quantitative analysis of surface arithmetic roughness, presented in Fig. 7C, further supports the observations from Fig. 7B, revealing distinct roughness evolution trends between the different formulations and models. For both formulations, a clear correlation between water content and roughness was observed. As the film transitioned from a highly hydrated state, a pronounced increase in roughness occurred due to structural rearrangements during moisture loss. However, as evaporation progressed further, roughness gradually decreased as the film compacted and stabilized. Interestingly, in the low coverage aged model, roughness remained higher than in the young model, as the underlying surface texture became more pronounced—a phenomenon not observed in the high-coverage formulation, where a more uniform film was maintained. These findings highlight the interplay between film coverage, evaporation rate, and surface roughness. Additionally, a transfer test was conducted by assessing the residue left on a cloth excised from a face mask—a material that frequently comes into contact with facial skin—after applying manual pressure for 2 s [38,42]. As shown in Fig. 7D, the low coverage cosmetic film exhibited significantly higher transfer, resulting in a more pronounced imprinting on the artificial skin surface. In addition, analysis of the cloth residues showed a cosmetic transfer covering 74% and 93% of the cloth area for the young and aged models, respectively. In contrast, the high coverage cosmetic film demonstrated significantly lower imprinting, primarily showing only the fiber patterns of the cloth on the artificial skin. The corresponding residue on the cloth was markedly reduced, covering 27% and 50% of the area for the young and aged models, respectively. The higher volatility of the low coverage film appears to contribute to increased morphological changes, particularly in aged skin models, whereas the high coverage film exhibits better film stability, which could translate to improved wearability in practical applications. Moreover, contact angle analysis in Fig. 8A revealed dynamic changes in the water-repelling properties of the outermost cosmetic film layer over time [43]. Initially, at 30 min post-deposition, both formulations exhibited moderate contact angles, indicating that the detected wettability can provide resistance to sweat and humidity, leading to longer wear while ensuring a good spreading and smooth finish. Interestingly, an increase in contact angle was observed at 60 min, suggesting a temporary enhancement of water repellency, potentially due to structural rearrangements or the continued evaporation of volatile components. However, by 24h, a marked decline in contact angle was evident, indicating a significant reduction in the film's hydrophobic properties. This effect is likely due to increased moisture absorption by the outermost layer of the dried film, which becomes more susceptible to water uptake as it loses its initial barrier properties, leading to a lower contact angle. Additionally, notable differences were observed between the low and high coverage formulations, which may be attributed to variations in surface composition, including emulsifiers, oils, and polymers. These findings suggest that the wettability of cosmetic films can be a crucial parameter to expect its longevity, spreadability and resistance. Finally, the adhesion strength of the formulations was evaluated under conditions simulating both passive water exposure (static immersion) and intense moisture stress combined with mechanical agitation (active immersion), addressing common concerns related to cosmetic performance, as shown in Fig. 8B [44,45]. Immersion tests in static and dynamic water conditions revealed significant differences in film retention between the young and aged models. Before immersion, both formulations appeared intact; however, after 30 min of static immersion, the aged model exhibited a more pronounced alteration in film morphology, characterized by the formation of blister-like deformations, suggesting an initial weakening of adhesion. Under active immersion conditions, where mechanical agitation was applied, the aged model experienced visible film detachment, particularly around the edges, indicating a higher susceptibility to water-induced adhesion loss. This suggests that, despite using the same formulation, the interaction between the film and the skin model is highly dependent on surface morphology. The increased roughness of the aged model likely promotes uneven material interactions, leading to heterogeneous adhesion strength and localized delamination. These findings emphasize the crucial role of skin texture and topography in determining formulation adherence. The greater susceptibility of the aged model to adhesion loss highlights the need for tailored formulations that account for variations in surface roughness, ensuring better durability and performance in real-world applications. Overall, the developed artificial skin models demonstrate strong potential for evaluating cosmetic film performance under physiologically relevant conditions, enabling the assessment of adhesion strength, moisture resistance, and wearability across different skin textures. Their ease of handling further enhances their reliability, providing a systematic and reproducible platform that minimizes errors and variability in cosmetic film testing.

3.5. Development of age-tailored porous artificial skin models

In addition to topography, the inherent complexity of the skin integrates various additional factors that can influence the deposition of cosmetic films. For example, the presence of sebum can exert a significant negative influence on the deposition of cosmetic films [9,38]. Sebum is a product of sebaceous glands composed of a mixture of lipids naturally produced by the human body. The sebaceous glands are connected to skin pores, from which they secrete and deposit sebum, which may surface on the outermost layer of the skin to provide protection and hydration. Depending on the area of the body, sweat can also be deposited within these pores [46]. Sebum production varies according to factors such as genetic background, gender, and age, leading to skin types that are often classified as "dry" or "oily". The account of the presence of sebum and the ability to modulate its levels within artificial skin models may show significance for a more accurate evaluation of the

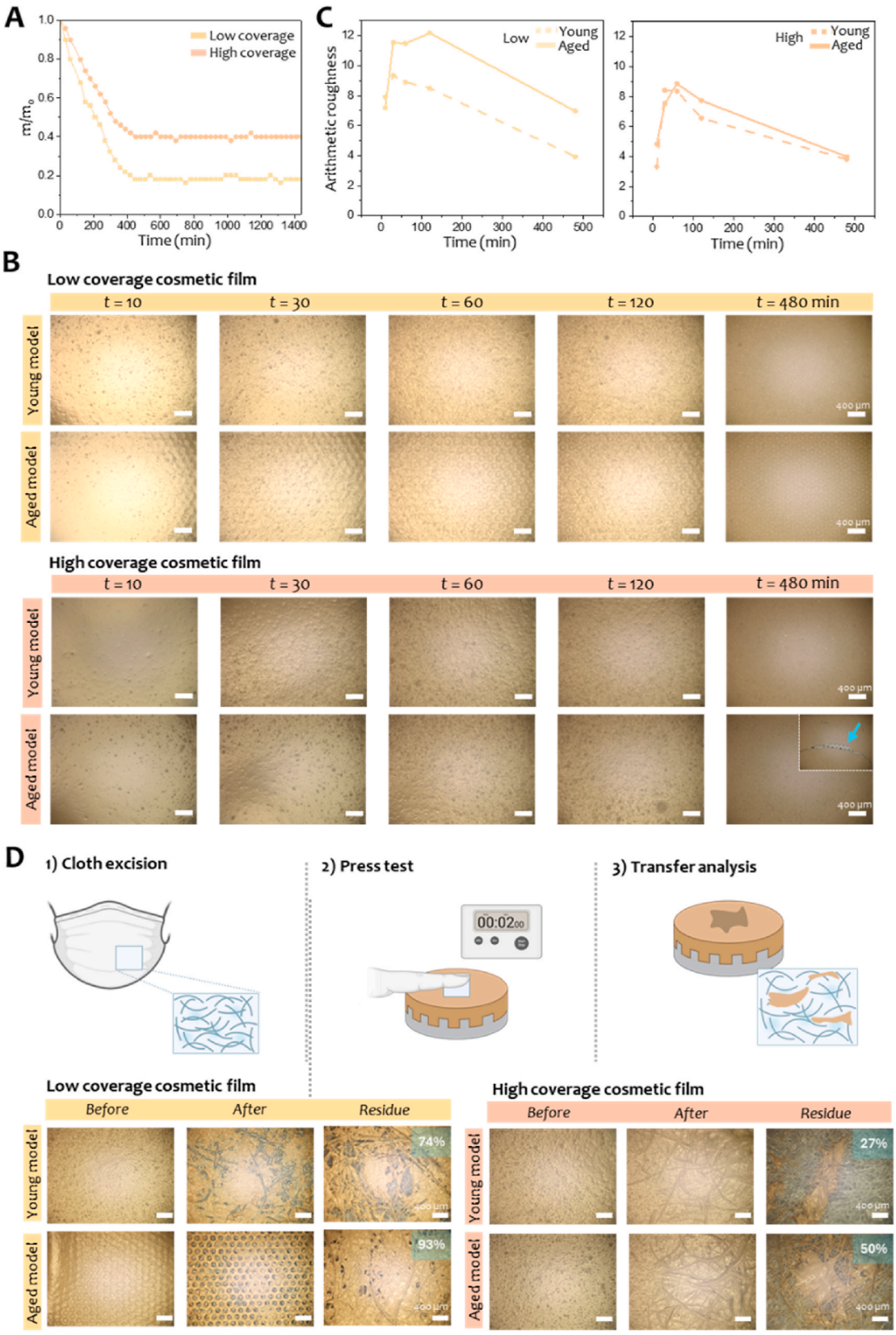

Fig. 7. Cosmetic film adhesion behavior. (A) Drying dynamics of the cosmetic formulations. (B) Time-dependent dynamics of the cosmetic films deposited on young and aged models observed with upright optical microscopy. The blue arrow indicates the presence of a crack in the film. (C) Cosmetic film arithmetic average roughness obtained from the surface analysis of the micrographs represented in (B). (D) Schematic illustration and micrographs of the before and after of a cosmetic transfer test carried out with the inner layer of a face mask. (For interpretation of the references to colour in this figure legend, the reader is referred to the Web version of this article.)

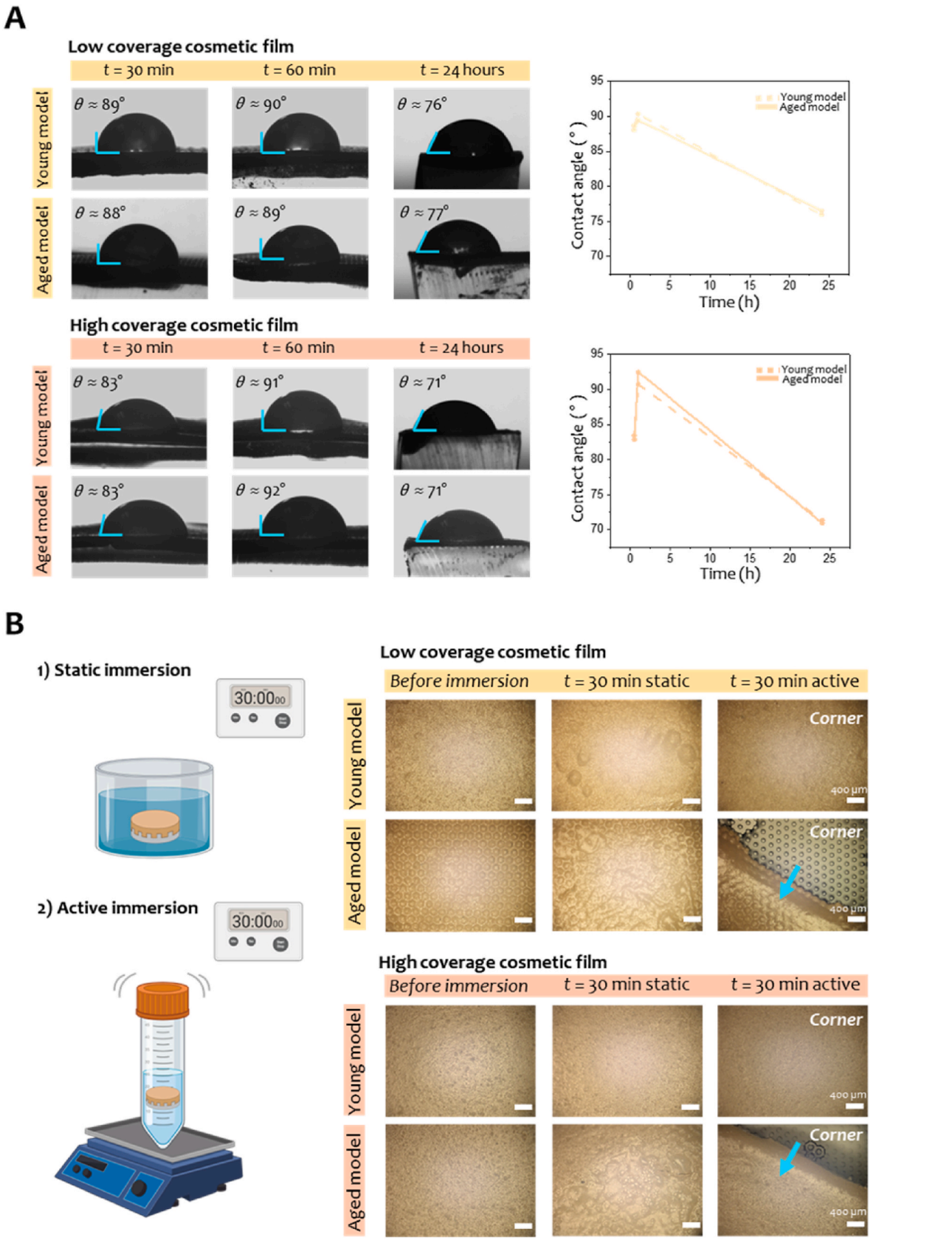

Fig. 8. Cosmetic film water resistance properties. (A) Contact angle measurement of the cosmetic film at different time stamps, for both low and high coverage formulations in young and aged skin models. (B) Schematic illustration and micrographs of the before and after of a water immersion test (static and active conditions). The blue arrows indicate the cosmetic film detachment and receding after active immersion on aged skin models. (For interpretation of the references to colour in this figure legend, the reader is referred to the Web version of this article.)

behavior of cosmetic films [38]. To further enhance the complexity of our age-tailored artificial platforms, porosity was incorporated to allow for sebum integration (Fig. 9A). To achieve this, citric acid crystals with an average size of 160 μm were incorporated into the PDMS mixture (see Supplementary Data Figs. S3A and S3B). The dissolution of the crystals within ethanol after PDMS curation facilitated the formation of networks of interconnected pores within the polymer matrices (Fig. 9B–Supplementary Data S3C and S3D). In these substrates, the pillars exhibited a more variable structure, with occasional depressions or protuberances, an effect caused by the incorporation of citric acid crystals.

The porosity of the substrates was calculated by segmentation of the three-dimensional datasets in two volumes, air and PDMS, obtaining an average porosity (V_P) of approximately 47% (Fig. 9C) [47]. The porosity and pore size achieved in the present artificial skin model are in the same range as the values previously described for the human acellular dermal matrix also measured by computed microtomography, highlighting the similarity of this designed model to the properties of real human skin [48]. Subsequently, the skin models were impregnated in a sebum mix comprising common lipids found in the human body and sweat, thus creating an artificial skin infused with sebum PDMS. Although sebum visualization by X-ray is difficult due to its comparable density with PDMS, sebum deposits were discernible on the surface of the skin models prior to the deposition of cosmetic films, as indicated by the yellow outline (Fig. 9D). This approach validates PDMS as an excellent material for the manufacture of artificial skin, allowing easy incorporation of pores within its bulk and the uptake of surrogate sebum mixtures. In the present work, a generalized approach was pursued to validate the potential of sebum incorporation in the present model and analyze its influence on cosmetic films. However, future fine-tuning of the porosity and sebum contents to mimic distinct skin types would be a necessary next step.

3.6. Impact of sebum in cosmetic film deposition

Finally, to evaluate the impact of sebum on the deposition of cosmetic films, porous skin models without and with sebum were coated with low and high coverage cosmetic formulations and subsequently analyzed. Visual analysis of the 3D segmented reconstructions of the porous models coated with low coverage films revealed that the inclusion of sebum resulted in a visibly smoother surface in both young and aged porous models (Fig. 10A). The X-Z cross-sections provided further evidence to support this observation, demonstrating a more uniform film deposition in the sebum-containing models. This is likely a result of sebum leading to excessive plasticization of the cosmetic film, making it more flexible, which consequently can lead to less wear due to weakened adhesion to the skin surface and easier transfer [9]. It should be noted that the presence of sebum resulted in distinct morphological changes within the formulation, particularly in the aged porous models, which showed a cosmetic film with compact stratified layers composed of high-density inclusions. This suggests that superficial sebum may have interacted with the formulation, altering its structural properties and leading to phase separation, with undesired consequences such as potential delamination [49]. In addition, sebum inclusion appeared to increase the thickness of the film, an effect that was more evident in the aged porous model. The quantification of the coverage provided further evidence of this distinction, demonstrating a significantly higher coverage deposition in the porous models with sebum. This was observed to be approximately 0.3-fold higher in the young porous model (Fig. 10B) and 0.4-fold higher in the aged porous model (Fig. 10C).

Furthermore, high coverage cosmetic films exhibited a more uniform surface in 3D segmented reconstructions of skin models containing

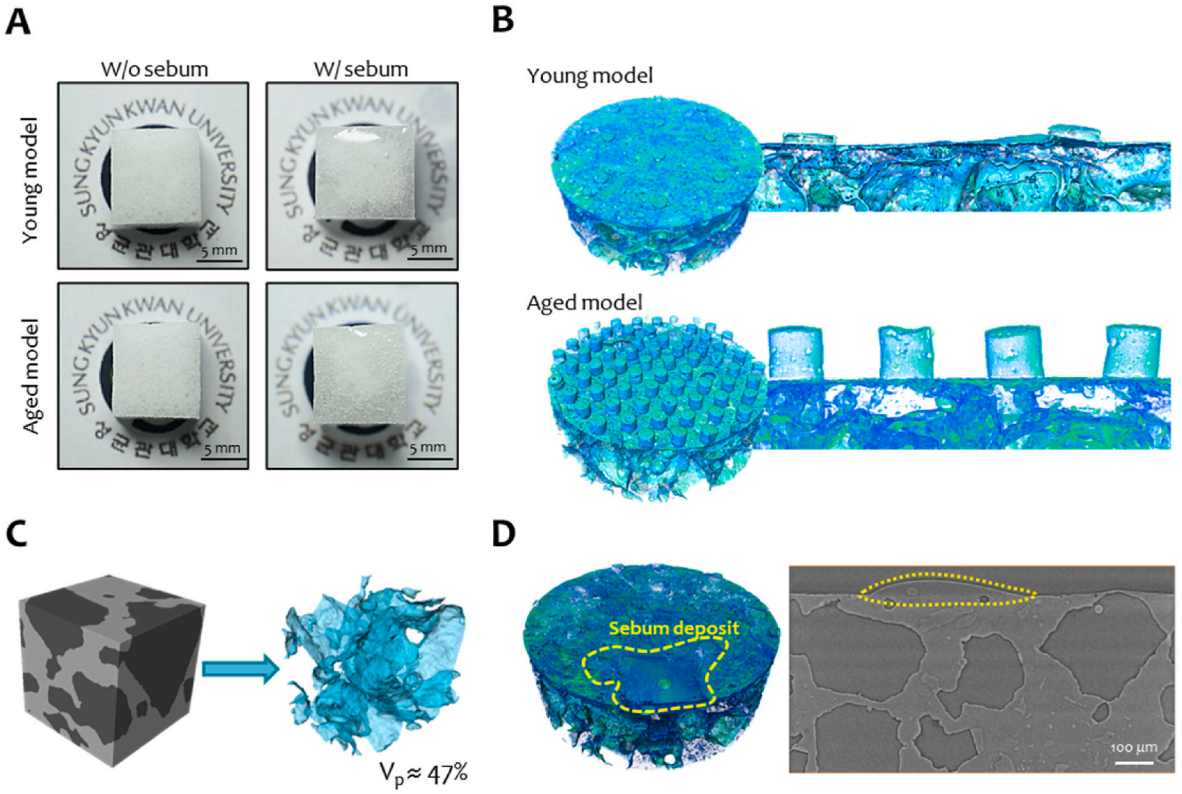

Fig. 9. Artificial porous skin model development. (A) Digital photographic representation of the young and aged porous artificial skin models before and after sebum inclusion. (B) Representative 3D microtomographs of young and aged porous artificial skin models. (C) Data segmentation for porosity quantification of the substrate. (D) Representative X-ray imaging of sebum deposit on the porous artificial skin, highlighted by the yellow outline. (For interpretation of the references to colour in this figure legend, the reader is referred to the Web version of this article.)

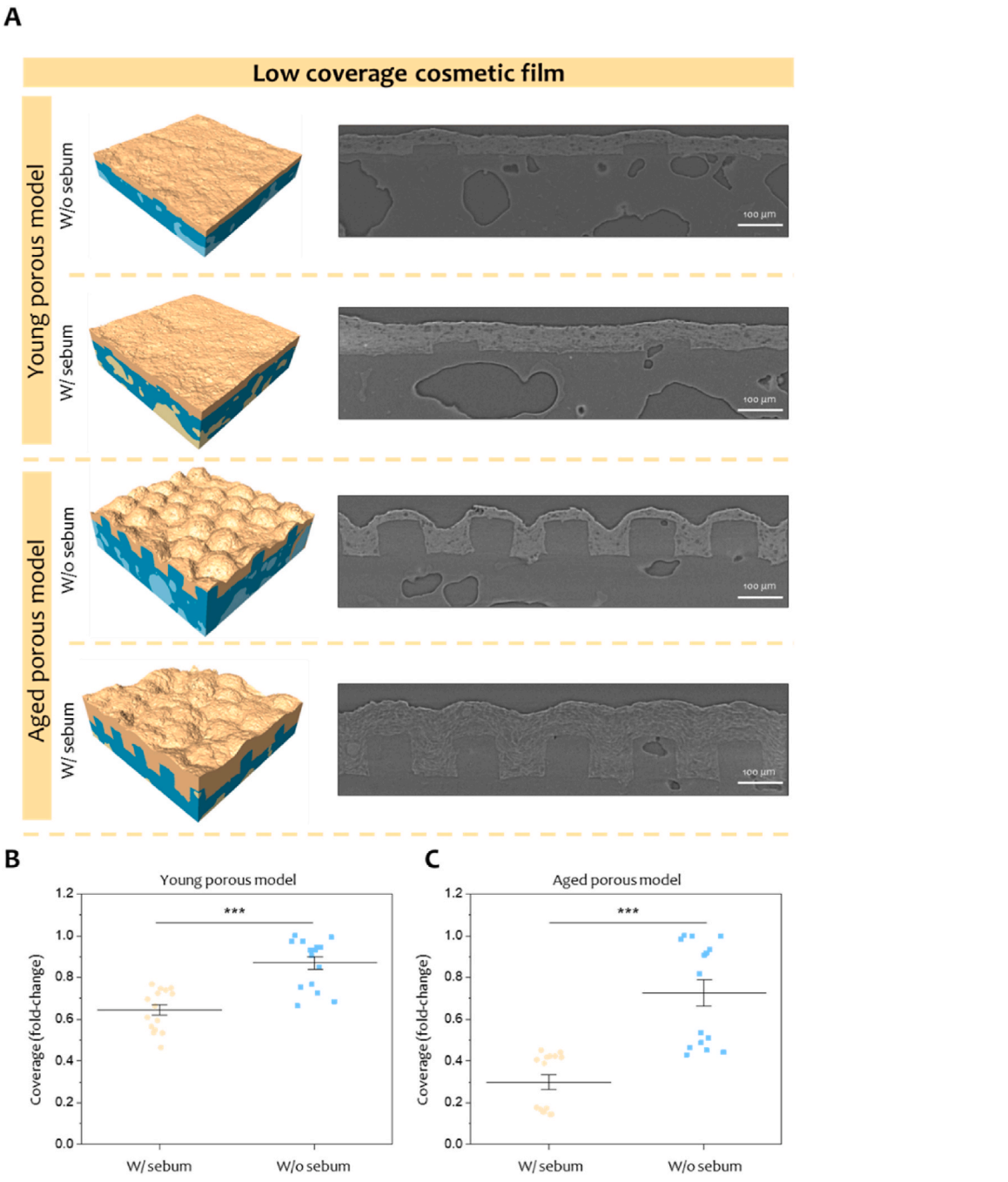

Fig. 10. Low coverage cosmetic film analysis in porous models. (A) Representative X-ray 3D reconstructions and X-Z cross-section slices of cosmetic film coverage in young and aged porous models without and with sebum. (B) and (C) Quantification of coverage thickness from X-Z cross section slices for young and aged porous models respectively.

sebum (Fig. 11A). However, this effect was less pronounced in the X-Z cross-section of the aged porous model, which exhibited a noticeably rough surface. Similarly to the low coverage films, the presence of sebum introduced distinct morphological changes in the formulation, along with an apparent increase in film thickness. Analysis of coverage thicknesses revealed significant differences in the presence of sebum. These differences were more pronounced in young porous models, exhibiting a 0.3-fold change (Fig. 11B), compared to aged porous models, which showed a 0.2-fold change in coverage thickness (Fig. 11C). This indicates that the impact of sebum depends on the characteristics and composition of each formulation, emphasizing the importance of considering these variables in the development of cosmetic products. As individuals with oily skin typically exhibit distinctive characteristics compared to those with dry skin, this model can provide a comprehensive understanding of how sebum affects the deposition of cosmetic films, leading to the negative effects commonly described by customers [38]. The coalescence of natural skin oils with emulsion droplets in formulations can provide insight into the visual discrepancies observed, which can result in instability and increased thickness in the product. However, due to the challenges associated with measuring skin oiliness and the use of X-ray imaging in this methodology, we were unable to compare these findings with real-world conditions. Therefore, further investigation is necessary to create more tailored sebum-dependent systems and clarify the impact of sebum on

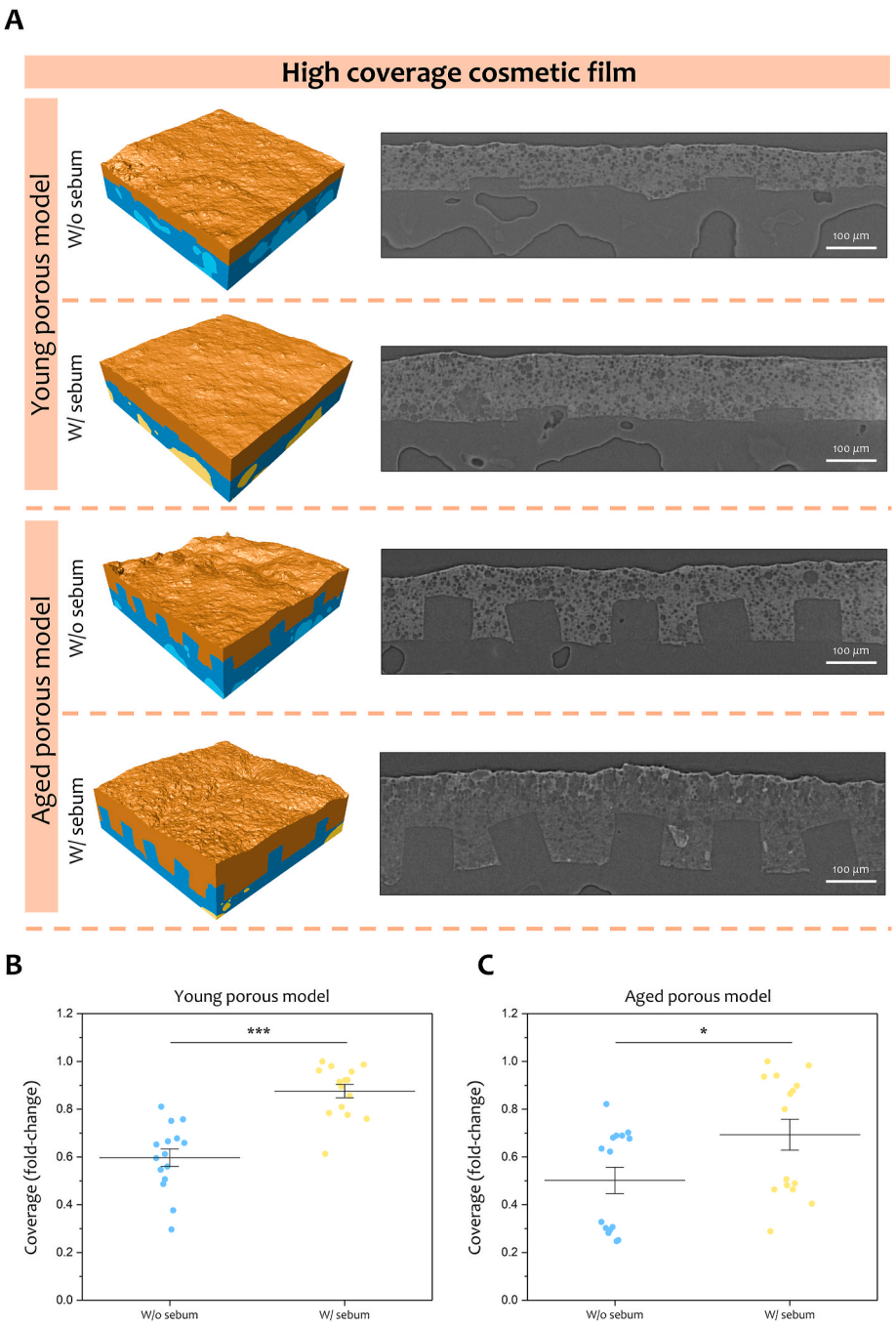

Fig. 11. High coverage cosmetic film analysis in porous models. (A) Representative X-ray 3D reconstructions and X-Z cross-section slices of cosmetic film coverage in young and aged porous models without and with sebum. (B) and (C) Quantification of coverage thickness from X-Z cross section slices for young and aged porous models respectively.

product deposition. A more thorough examination of this subject, particularly the modulation of oiliness in accordance with real-life conditions, is imperative for a comprehensive understanding of product performance.

4. Conclusions

The cosmetic market is in continuous expansion, marked by the ongoing development of innovative products to meet increasing consumer demands. This significant growth emphasizes the commitment of the cosmetic industry to improving product quality and maintaining competitiveness, requiring continuous expansion and technological development to appeal to consumers. The role of skin characteristics such as topography or roughness in the application and performance of cosmetic films represents a significant factor in the field of cosmetic formulation. The artificial skin models developed in the present work exhibited a noteworthy correlation with real skin, demonstrating comparability for the analysis of the tested formulations while prioritizing the use of low-cost components and ease of assembly. Thus, we highlight the role of age as a crucial determinant in product development and the necessity of developing cosmetic products that are tailored to specific target demographics. Furthermore, this work underscores the potential of advanced skin models to minimize the dependence on animal testing, providing a more reproducible and targeted methodology

for the assessment of cosmetic formulations. Future research should focus on developing a more sophisticated model that takes into account skin porosity and the varying levels of sebum to align with real-world oil production by different types of skin. This versatile, biocompatible platform also holds promise as a scaffold to accommodate skin cell culture, further expanding its applications beyond cosmetic research, such as drug screening and disease treatment.

CRediT authorship contribution statement

Marta Gonçalves: Writing – original draft, Methodology, Investigation, Conceptualization. **Sofia Brito:** Writing – original draft, Methodology, Investigation, Conceptualization. **Chaeyeon Song:** Investigation. **Youngkyu Han:** Investigation. **Bum-Ho Bin:** Investigation. **Byung Mook Weon:** Writing – review & editing, Supervision, Funding acquisition, Conceptualization.

Declaration of competing interest

The authors declare that they have no known competing financial interests or personal relationships that could have appeared to influence the work reported in this paper.

Acknowledgements

This research has been supported by AMOREPACIFIC and by Yangyoung Foundation in 2024. Additionally, this work was supported by the National Research Foundation of Korea (NRF) grant funded by the Korea government (MSIT) (No. RS-2024-00405818) and funded by the Ministry of Education (2019R1A6A1A0303321522).

Appendix A. Supplementary data

Supplementary data to this article can be found online at https://doi.org/10.1016/j.mtbio.2025.101618.

Data availability

Data will be made available on request.

References

[1] C.D. Dimitrakopoulos, P.R. Malenfant, Organic thin film transistors for large area electronics, Adv. Mater. 14 (2) (2002) 99–117.
[2] D. Zacher, O. Shekhah, C. Wöll, R.A. Fischer, Thin films of metal–organic frameworks, Chem. Soc. Rev. 38 (5) (2009) 1418–1429.
[3] W.-H. Chou, A. Gamboa, J.O. Morales, Inkjet printing of small molecules, biologics, and nanoparticles, Int. J. Pham. 600 (2021) 120462.
[4] S. Karki, H. Kim, S.-J. Na, D. Shin, K. Jo, J. Lee, Thin films as an emerging platform for drug delivery, Asian J. Parm, Science 11 (5) (2016) 559–574.
[5] I.C. Libio, R. Demori, M.F. Ferrão, M.I. Lionzo, N.P. da Silveira, Films based on neutralized chitosan citrate as innovative composition for cosmetic application, Mater. Sci. Eng. C 67 (2016) 115–124.
[6] A. Sionkowska, K. Lewandowska, M. Kurzawa, Chitosan-based films containing rutin for potential cosmetic applications, Polymers 15 (15) (2023) 3224.
[7] M. Pensalfini, M. Rotach, R. Hopf, A. Bielicki, R. Santoprete, E. Mazza, How cosmetic tightening products modulate the biomechanics and morphology of human skin, Acta Biomater. 115 (2020) 299–316.
[8] D. Mendoza, M. Maliha, V. Raghuwanshi, C. Browne, L. Mouterde, G. Simon, F. Allais, G. Garnier, Diethyl sinapate-grafted cellulose nanocrystals as nature-inspired UV filters in cosmetic formulations, Mater. Today Bio. 12 (2021) 100126.
[9] Z. Li, H.S. Bui, Factors affecting cosmetics adhesion to facial skin, Surface Science and Adhesion in Cosmetics (2021) 543–584.
[10] M. De Melo, P. Maia Campos, Application of biophysical and skin imaging techniques to evaluate the film-forming effect of cosmetic formulations, Int. J. Cosmet. Sci. 41 (6) (2019) 579–584.
[11] L. Gilbert, G. Savary, M. Grisel, C. Picard, Predicting sensory texture properties of cosmetic emulsions by physical measurements, Chemometr. Intell. Lab. Syst. 124 (2013) 21–31.
[12] G.J. Fisher, S. Kang, J. Varani, Z. Bata-Csorgo, Y. Wan, S. Datta, J.J. Voorhees, Mechanisms of photoaging and chronological skin aging, Arch. Dermatol. 138 (11) (2002) 1462–1470.
[13] S. Askaruly, Y. Ahn, H. Kim, A. Vavilin, S. Ban, P.U. Kim, S. Kim, H. Lee, W. Jung, Quantitative evaluation of skin surface roughness using optical coherence tomography in vivo, IEEE J. Sel. Top. Quant. Electron. 25 (1) (2018) 1–8.
[14] G. Carlos da Silva, M.B. Barbosa, F.B.C. Júnior, P.L. Moreira, R. Werka, A. A. Martin, Detection of skin wrinkles and quantification of roughness using a novel image processing technique from a dermatoscope device, Skin Res. Technol. 29 (6) (2023) e13335.
[15] H. Jo, S. Brito, B.M. Kwak, S. Park, M.-G. Lee, B.-H. Bin, Applications of mesenchymal stem cells in skin regeneration and rejuvenation, Int. J. Mol. Sci. 22 (5) (2021) 2410.
[16] S. Brito, M. Baek, B.-H. Bin, Skin structure, physiology, and pathology in topical and transdermal drug delivery, Pharmaceutics 16 (11) (2024) 1403.
[17] X. Dan, S. Li, H. Chen, P. Xue, B. Liu, Y. Ju, L. Lei, Y. Li, X. Fan, Tailoring biomaterials for skin anti-aging, Mater. Today Bio. (2024) 101210.
[18] A. Sakdinawat, D. Attwood, Nanoscale X-ray imaging, Nat. Photonics 4 (12) (2010) 840–848.
[19] G. Perfetti, E. Van de Casteele, B. Rieger, W.J. Wildeboer, G.M. Meesters, X-ray micro tomography and image analysis as complementary methods for morphological characterization and coating thickness measurement of coated particles, Adv. Powder Technol. 21 (6) (2010) 663–675.
[20] S. Yoon, M. Seok, M. Kim, Y.H. Cho, Wearable porous PDMS layer of high moisture permeability for skin trouble reduction, Sci. Rep. 11 (1) (2021) 938.
[21] M. Gonçalves, J.Y. Kim, Y. Kim, N. Rubab, N. Jung, T. Asai, S. Hong, B.M. Weon, Droplet evaporation on porous fabric materials, Sci. Rep. 12 (1) (2022) 1087.
[22] H. Kim, M. Gonçalves, S.H. Kang, B.M. Weon, High density deposits of binary colloids, Sci. Rep. 12 (1) (2022) 22307.
[23] T. Nagaoka, Y. Kimura, Quantitative cosmetic evaluation of long-lasting foundation using multispectral imaging, Skin Res. Technol. 25 (3) (2019) 318–324.
[24] W. Montagna, The Structure and Function of Skin, Elsevier, 2012.
[25] G. Honari, Skin structure and function. Sensitive Skin Syndrome, CRC Press, 2017, pp. 16–22.
[26] Z. Al-Khafaji, S. Brito, B.-H. Bin, Zinc and zinc transporters in dermatology, Int. J. Mol. Sci. 23 (24) (2022) 16165.
[27] S. Brito, H. Heo, J. Kim, B. Cha, Y. Jeong, W. Choi, C. Shrestha, G.H. Lee, S.J. Park, K.B. Yoon, Age-associated interplay between zinc deficiency and Golgi stress hinders microtubule-dependent cellular signaling and epigenetic control, Dev. Cell (2025).
[28] T. Weng, P. Wu, W. Zhang, Y. Zheng, Q. Li, R. Jin, H. Chen, C. You, S. Guo, C. Han, Regeneration of skin appendages and nerves: current status and further challenges, J. Transl. Med. 18 (2020) 1–17.
[29] J.G. Diosa, R. Moreno, E.L. Chica, J.A. Villarraga, A.B. Tepole, Changes in the three-dimensional microscale topography of human skin with aging impact its mechanical and tribological behavior, PLoS One 16 (7) (2021) e0241533.
[30] L. Li, S. Mac-Mary, D. Marsaut, J.M. Sainthillier, S. Nouveau, T. Gharbi, O. de Lacharriere, P. Humbert, Age-related changes in skin topography and microcirculation, Arch. Dermatol. Res. 297 (2006) 412–416.
[31] J. Lagarde, C. Rouvrais, D. Black, Topography and anisotropy of the skin surface with ageing, Skin Res. Technol. 11 (2) (2005) 110–119.
[32] C. Trojahn, G. Dobos, M. Schario, L. Ludriksone, U. Blume-Peytavi, J. Kottner, Relation between skin micro-topography, roughness, and skin age, Skin Res. Technol. 21 (1) (2015) 69–75.
[33] H. Zahouani, M. Djaghloul, R. Vargiolu, S. Mezghani, M. Mansori, Contribution of human skin topography to the characterization of dynamic skin tension during senescence: morpho-mechanical approach. J. Phys.: Conf. Ser., IOP Publishing, 2014 012012.
[34] L.-C. Gerhardt, A. Schiller, B. Müller, N. Spencer, S. Derler, Fabrication, characterisation and tribological investigation of artificial skin surface lipid films, Tribol. Lett. 34 (2009) 81–93.
[35] F. Eudier, M. Grisel, G.r. Savary, C.l. Picard, Design of a lipid-coated polymeric material mimic human skin surface properties: a performing tool to evaluate skin interaction with topical products, Langmuir 36 (17) (2020) 4582–4591.
[36] H.S. Bui, D. Coleman-Nally, Film-forming technology and skin adhesion in long-wear cosmetics. Adhesion in Pharmaceutical, Biomedical and Dental Fields, 2017, pp. 141–166.
[37] G.S. Luengo, H.S. Bui, J. Portal, Formation and performance of cosmetic films in cosmetics. Handbook of Cosmetic Science and Technology, CRC Press, 2022, pp. 167–181.
[38] J.V. Badami, H.S. Bui, Quantification of the color transfer from long-wear face foundation products: the relevance of wettability, Surface Science and Adhesion in Cosmetics (2021) 379–399.
[39] E. Sutterby, P. Thurgood, S. Baratchi, K. Khoshmanesh, E. Pirogova, Microfluidic skin-on-a-chip models: toward biomimetic artificial skin, Small 16 (39) (2020) 2002515.
[40] S. Lee, J. Baek, M. Shin, J. Koh, The quantitative analysis of spreadability, coverage, and adhesion effect after application of the base make-up product, Skin Res. Technol. 20 (3) (2014) 341–346.
[41] G. Puccetti, Water-resistant sunscreens for skin protection: an in vivo approach to the two sources of sunscreen failure to maintain UV protection on consumer skin, Int. J. Cosmet. Sci. 37 (6) (2015) 613–619.
[42] E. Yokoyama, K. Udodaira, A. Nicolas, E. Yamashita, A. Maudet, F. Flament, D. Velleman, A preliminary study to understand the effects of mask on tinted face cosmetics, Skin Res. Technol. 27 (5) (2021) 797–802.
[43] R. Hagens, T. Mann, V. Schreiner, H. Barlag, H. Wenck, K.P. Wittern, W. Mei, Contact angle measurement–a reliable supportive method for screening water-resistance of ultraviolet-protecting products in vivo, Int. J. Cosmet. Sci. 29 (4) (2007) 283–291.

[44] C. Pang, H.S. Bui, Adhesion aspect in semi-permanent mascara, Surface Science and Adhesion in Cosmetics (2021) 585–633.
[45] H.S. Bui, M. Hasebe, J. Ebanks, Evaluation of sebum resistance for long-wear face make-up products using contact angle measurements, Advances in Contact Angle, Wettability and Adhesion 4 (2019) 193–221.
[46] F. Flament, G. Francois, H. Qiu, C. Ye, T. Hanaya, D. Batisse, S. Cointereau-Chardon, M.D.G. Seixas, S.E. Dal Belo, R. Bazin, Facial skin pores: a multiethnic study, Clin. Cosmet. Invest. Dermatol. (2015) 85–93.
[47] M. Gonçalves, B.M. Weon, Evaluating droplet survivability on face masks with X-ray microtomography, ACS Appl. Bio Mater. 7 (1) (2023) 193–202.
[48] Y. Wang, R. Xu, W. He, Z. Yao, H. Li, J. Zhou, J. Tan, S. Yang, R. Zhan, G. Luo, Three-dimensional histological structures of the human dermis, Tissue Eng. C Methods 21 (9) (2015) 932–944.
[49] Z. Li, B. Maxon, K. Nguyen, M. Lee, M. Gu, P. Pretzer, A general formulation strategy toward long-wear color cosmetics with sebum resistance, J. Cosmet. Sci. 68 (1) (2017) 91–98.